crystals

MDPI

Article

Anisotropic Surface Formation Based on Brush-Coated Nickel-Doped Yttrium Oxide Film for Enhanced Electro-Optical Characteristics in Liquid Crystal Systems

Dong-Wook Lee [1], Da-Bin Yang [1], Dong-Hyun Kim [1], Jin-Young Oh [1], Yang Liu [2,*] and Dae-Shik Seo [1,*]

[1] IT Nano Electronic Device Laboratory, Department of Electrical and Electronic Engineering, Yonsei University, 50 Yonsei-ro, Seodaemun-gu, Seoul 03722, Korea
[2] College of Information Science and Technology, Donghua University, 2999 North Renmin Road, Songjiang District, Shanghai 201620, China
* Correspondence: liuyang@dhu.edu.cn (Y.L.); dsseo@yonsei.ac.kr (D.-S.S.)

Abstract: This paper introduces anisotropic nickel yttrium oxide (NYO) film formed by the brush coating technique. X-ray photoelectron spectroscopy confirmed well-formed NYO film after the curing process, and the morphology of the surface was investigated using atomic force microscopy. The shear stress driven from brush hair movements caused the nano/micro-grooved anisotropic surface structure of NYO. This anisotropic surface induced uniform liquid crystal (LC) alignment on the surface, which was confirmed by pre-tilt angle analysis and polarized optical microscopy. The contact angle measurements revealed an increase in hydrophilicity at higher temperature curing, which contributed to homogenous LC alignment. The NYO film achieved good optical transmittance and thermal stability as an LC alignment layer. In addition, the film demonstrated good electro-optical properties, stable switching, and significantly enhanced operating voltage performance in a twisted-nematic LC system. Therefore, we expect that this brush coating method can be applied to various inorganic materials to achieve an advanced LC alignment layer.

Keywords: brush coating; nickel yttrium oxide; surface morphology; liquid crystal; low voltage operation

Citation: Lee, D.-W.; Yang, D.-B.; Kim, D.-H.; Oh, J.-Y.; Liu, Y.; Seo, D.-S. Anisotropic Surface Formation Based on Brush-Coated Nickel-Doped Yttrium Oxide Film for Enhanced Electro-Optical Characteristics in Liquid Crystal Systems. *Crystals* **2022**, *12*, 1554. https://doi.org/10.3390/cryst12111554

Academic Editors: Zhenghong He and Yuriy Garbovskiy

Received: 13 October 2022
Accepted: 29 October 2022
Published: 31 October 2022

1. Introduction

With the rapid development of surface engineering, interest in highly functional and economical devices is increasing in the optical, electronic, and display industries. Liquid crystals (LCs) are versatile materials that can be applied to many industries due to their unique properties, such as the intermediate state of liquid and solid, refractive anisotropy, and dielectric anisotropy [1–3]. In particular, LC displays (as a representative application of using LCs) have received significant attention due to their durability, excellent electro-optical (EO) properties, and high resolution [4–7]. For high-performance LC-based devices, uniform LC alignment should be achieved. This is because the LCs that uniformly aligned can control the light with high reliability, whereas irregularly distributed LCs cause the light leakage effect and unstable EO properties, which can deteriorate device performance [8,9]. Accordingly, LCs are located on the alignment layer, where the alignment state is affected by interactions between the LCs and the alignment layer.

Various treatments have been researched for the alignment layer to induce uniform LC alignment, including the rubbing method [10,11], ultraviolet photoalignment [12], oblique deposition [13], and plasma treatment [14]. Especially the method called rubbing has been extensively adopted in industry because of its simple and cost-effective properties. In this method, anisotropic microgrooves are produced on the alignment layer surface through contact with a high-speed rotating fabric roller to induce uniform LC alignment. However, this intense mechanical contact also causes cracks, local defects, and electrostatic problems, resulting in a breakdown of device performance [15].

Herein, we introduce the brush coating technique to induce uniform LC orientation on the alignment layer. This method is very convenient and can integrate the film formation process and treatment process for alignment layer, resulting in high throughput and cost-effectiveness. Moreover, this solution-based brush coating method can induce shear stress to the solution (by brush hair sweeping) and a retracing force on the deposited solution. We assumed that this shear stress could generate a directional distribution of the solution and the subsequent rapid heat application could form the anisotropic microgroove film surface with the sol-gel method. Nickel yttrium oxide (NYO) was used for the alignment layer due to its good dielectric characteristics, which means the potential of EO performance as an alignment layer [16,17]. The sol-gel-based brush coating method was adopted with a glass substrate, and the film curing temperature was varied. The film surface morphology was verified by atomic force microscopy (AFM). X-ray photoelectron spectroscopy (XPS) verified the well-formed NYO film state. Optical transparency of the layer was confirmed by ultraviolet-visible-near infrared (UV-vis-NIR) spectroscopy, and the atomic structural properties were verified by X-ray diffraction (XRD). In addition, contact angle investigation was conducted to verify the chemical affinity of the film surface. The LC orientation state was confirmed by polarized optical microscopy (POM) and pre-tilt angle analysis, and the EO characteristics of the film were examined in a twisted-nematic (TN) LC system.

2. Materials and Methods

To form the NYO film, 2 cm × 3 cm glass substrates were prepared. They were cleaned by the sonification method using isopropyl alcohol and acetone. The substrates were treated in each solvent for 10 min with subsequent drying with N_2 gas. The 0.1 M NYO solution was then produced by mixing nickel(II) chloride hydrate and yttrium(III) nitrate hexahydrate at a ratio of 1:9 in a 2-methoxyethanol solvent. The mixed solution was then stirred at 430 rpm for 2 h at 75 °C and then aged for at least 24 h. The used metal mateials are for the sol-gel process, and thus the sol state of NYO is uniformly distributed in the solution. The prepared brush hair was saturated in the solution and the combing of the hair on the prepared glass substrate produced the film deposition process. Subsequently, the curing process was enacted under 70, 150, and 230 °C conditions. The curing made sol-gel transition, with decomposing and hardening the oxide material, and formed the NYO film.

Stoichiometric differences of the brush-coated NYO films (depending on curing temperature) were examined by XPS (K-alpha, Thermo Scientific, Waltham, MA, USA). A monochromatic Al X-ray source (Al Ka line:1486.6 eV) was used with a 12 kV/3 mA power source. The surface morphology information of the film surface was investigated using AFM (NX-10, Park Systems, Seoul, Korea) and corresponding line profile data. The dektakXT stylus profiler (Bruker, Billerica, MA, USA) was used for measuring the NYO film thickness with 2 μm radius tip. The thickness was measured to 243.32 nm. The optical transmittance of the film was then evaluated with UV-Vis-NIR spectroscopy (JASCO Corporation, V-650, Tokyo, Japan) using a wavelength range of 250–850 nm. Using the measurement result in air as a baseline, the transmittance of the glass substrate, the indium-tin-oxide (ITO)-coated glass substrate, and the NYO film coated glass substrate were measured, respectively. The surface chemical affinity of the film was examined through contact angle measurements using the sessile drop technique with deionized water and diiodomethane. A phoenix 300 surface angle analyzer and the IMAGE PRO 300 software were used for the analyses. The atomic structural properties of the film were examined by XRD (DMAX-IIIA, Rigaku, Tokyo, Japan) with a 2-theta range of 20–80°.

To verify the LC alignment state on the brush-coated NYO film, anti-parallel (AP) cells were assembled by the brush-coated NYO films, which were cured at various temperatures. The cell gap was uniformly assembled to 60 μm, and then positive nematic LCs (IAN-5000XX T14, $T_{N\rightarrow I}$ = 81.8 °C, Δn = 0.111, ne = 1.595, no = 1.484; JNC) were injected into the cells by syringes via capillary force. The assembled LC cells were observed by POM (BXP 51, Olympus, Tokyo, Japan) to confirm the LC alignment state, and the pre-tilt of the LCs in the cell was investigated using the crystal rotation method (Autronic TBA 107).

Thermal stability to LC alignment was inspected by the annealing process and subsequent POM measurements. To examine the EO properties, a TN-LC cell was assembled with a uniform cell gap of 5 μm. The response time-transmittance (R-T) and voltage-transmittance (V-T) graphs were measured using the LCD evaluation system (LCMS-200) to confirm the switching and operating voltage characteristics.

3. Results and Discussion

As illustrated in Figure 1, brush hair movement during the brush coating process was expected to form directional NYO precursor distribution on the substrate via shear stress, which originated from the retracing force on the deposited bulk solution [18,19]. This sol state of the NYO could be transformed into a gel state during the curing process, forming a directional NYO film structure on the surface.

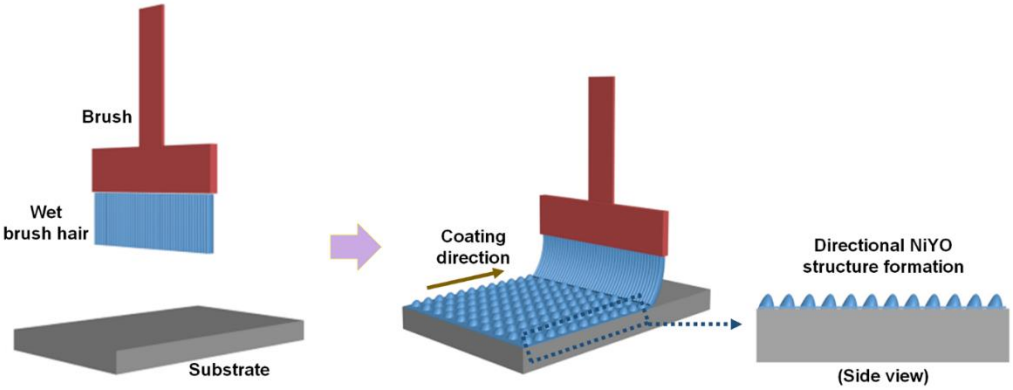

Figure 1. Brush coating process illustration and the expected structure of nickel yttrium oxide film after the curing process.

To verify the morphology of the NYO film, AFM measurements, and corresponding line profile analyses were conducted, as depicted in Figure 2. When the curing process progressed at 70 and 150 °C, some large lumps were measured on the surface that were attributed to large NYO particles between the brush hairs, although neither sample exhibited any distinct structural property with irregular morphology. The corresponding line profiles also denoted an irregular structure, which could not be perceived as anisotropic morphology. In contrast, the 230 °C cured sample exhibited an anisotropic structure that was aligned in a single direction, similar to the brush coating direction in the AFM result. In terms of line profile, the surface exhibited an anisotropic micro/nano-groove structure in which the height increased and decreased repeatedly according to the direction of brush coating. This anisotropic structure originated from the NYO precursors that were distributed during the brush coating process [20]. From these results, it was demonstrated that curing temperature is the important factor when forming an anisotropic NYO film structure while maintaining the directional property of the NYO precursors. In addition, the application of sufficiently high temperature should be guaranteed to ensure rapid transformation of the NYO sol state to a gel state. When the curing temperature was too low, sufficient transformation did not occur and unstable films were formed under the influence of residual solvent.

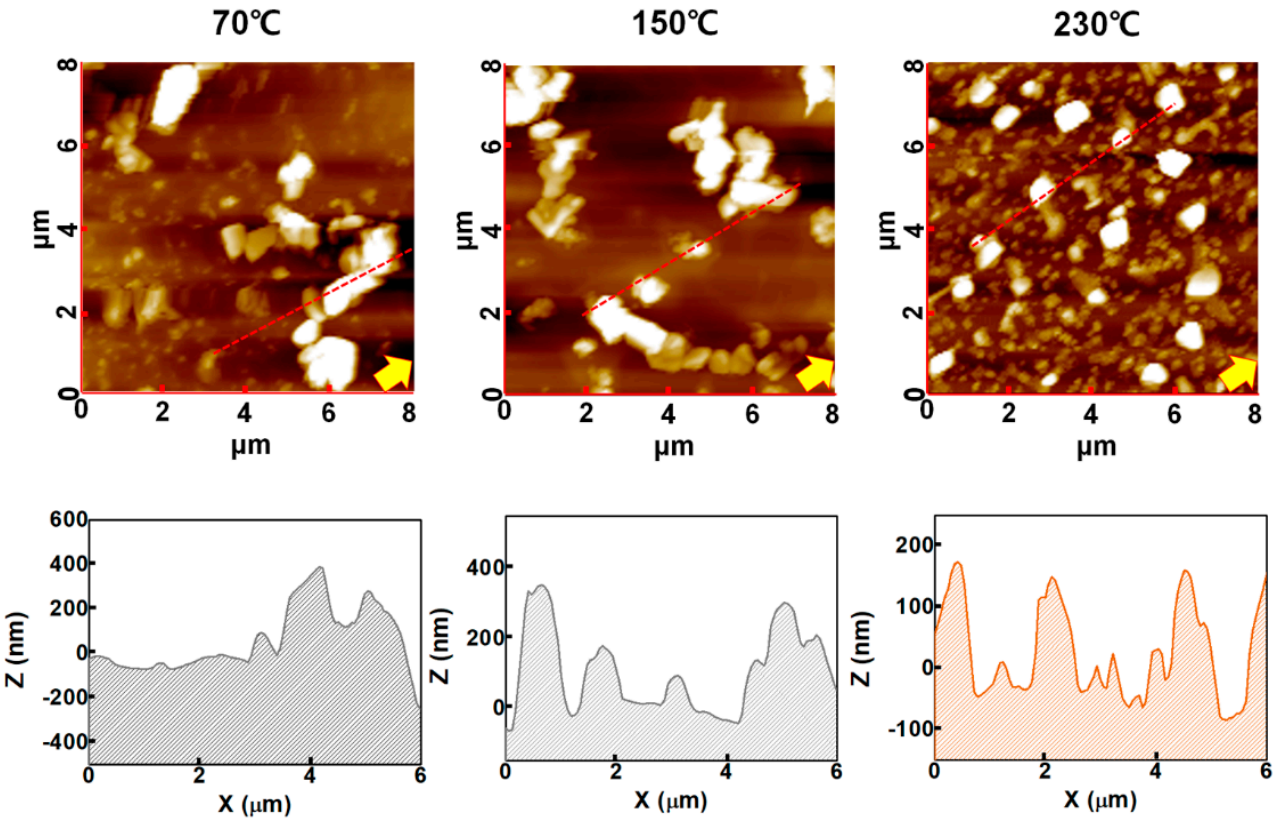

Figure 2. Atomic force microscopy images and corresponding line profiles of the brush−coated nickel yttrium oxide films cured at 70, 150, and 230 °C (The red dotted line corresponds to the line profile data). Direction of brush coating is denoted by a yellow arrow.

The stoichiometric difference between the 70 and 230 °C cured NYO films was investigated by XPS analysis, from which the Ni 2p, Y 3d, and O 1s core-level spectra were obtained (Figure 3). In the Ni 2p spectra, both samples revealed four sub-peaks, representing Ni 2p3/2, Ni 2p1/2, and two satellites. The 3/2 and 1/2 peaks were respectively centered at 854.46 and 872.13 eV for the 70 °C sample, compared to 854.38 and 871.85 eV for the 230 °C sample. The Y 3d spectra comprised two sub-peaks, which represented Y 3d5/2 and Y 3d3/2 in each for both samples. Each peak was centered at 157.89 and 159.84 eV for the 70 °C sample compared to 157.23 and 158.88 eV for the 230 °C sample. The O 1s spectra comprised two sub-peaks, each indicating metal-oxide bonding and oxygen vacancy. These peaks were centered in the ranges of 528.50–530.00 eV and 531.00–531.50 eV, respectively. The peak intensity increases of Ni 2p, Y 3d, and metal-oxide bonding as the curing temperature is increased from 70 to 230 °C indicated that thermal oxidation was well-progressed at the higher curing temperature [21]. This contributed to the formation of a stable NYO film during the curing process, although 70 °C curing was relatively insufficient for producing a stable oxidized NYO film structure, as confirmed by the AFM analysis.

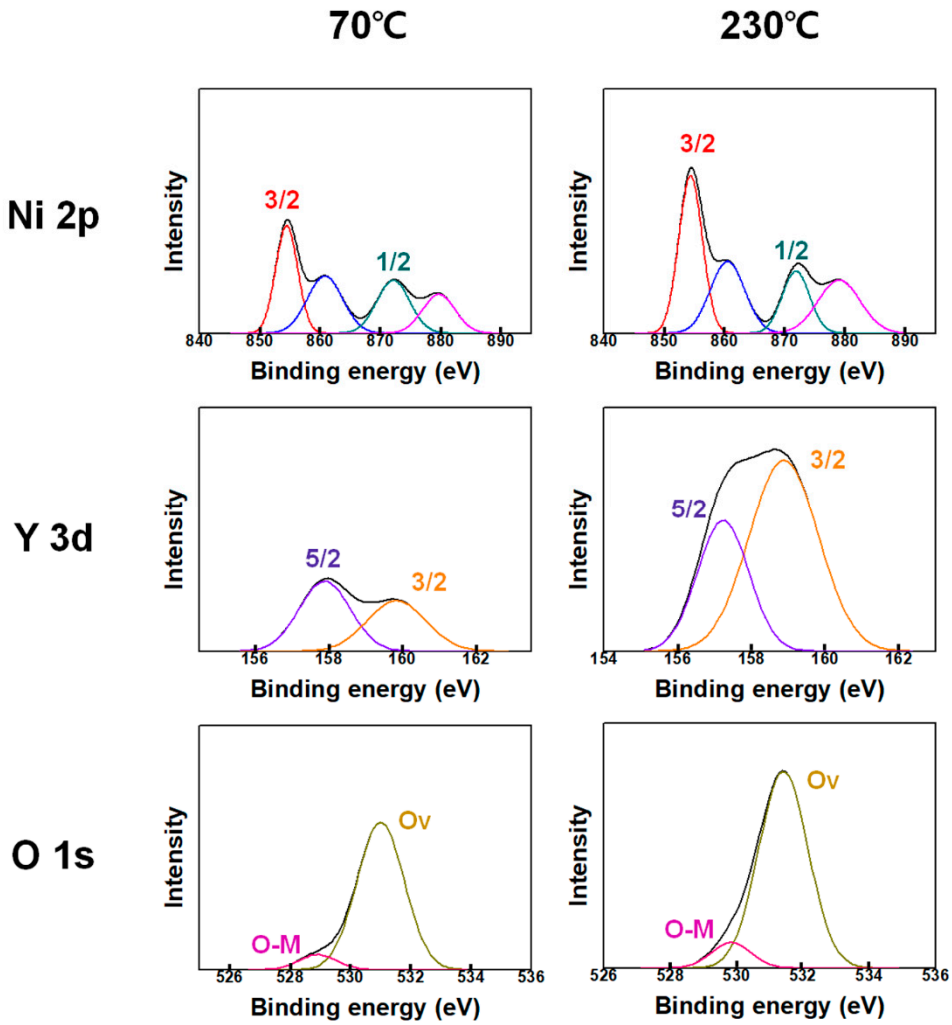

Figure 3. X-ray photoelectron spectroscopy results of Ni 2p, Y 3d, and O1s core levels obtained from brush-coated nickel yttrium oxide films which were cured at 70 and 230 °C.

To verify the adoptability of the brush-coated NYO film to the LC alignment layer, the film's optical transparency was measured (Figure 4). In addition, the transparency of plain and ITO coated glasses were obtained for comparison. The 70 and 150 °C cured films exhibited significantly lower transmittance curves compared to the 230 °C cured film. This confirmed that the optical properties of the 70 and 150 °C cured samples were deteriorated by the residual-solvent effect, whereas the 230 °C cured sample achieved a stable film state in terms of optical properties. The average transmittance of the 230 °C cured sample was 85.9% in the visible region (380–740 nm wavelength in this study). Considering that the corresponding values for the plain and ITO glasses were 86.5% and 82.3%, respectively, it was verified that the 230 °C cured brush-coated NYO film has the potential to be adopted as an LC alignment layer.

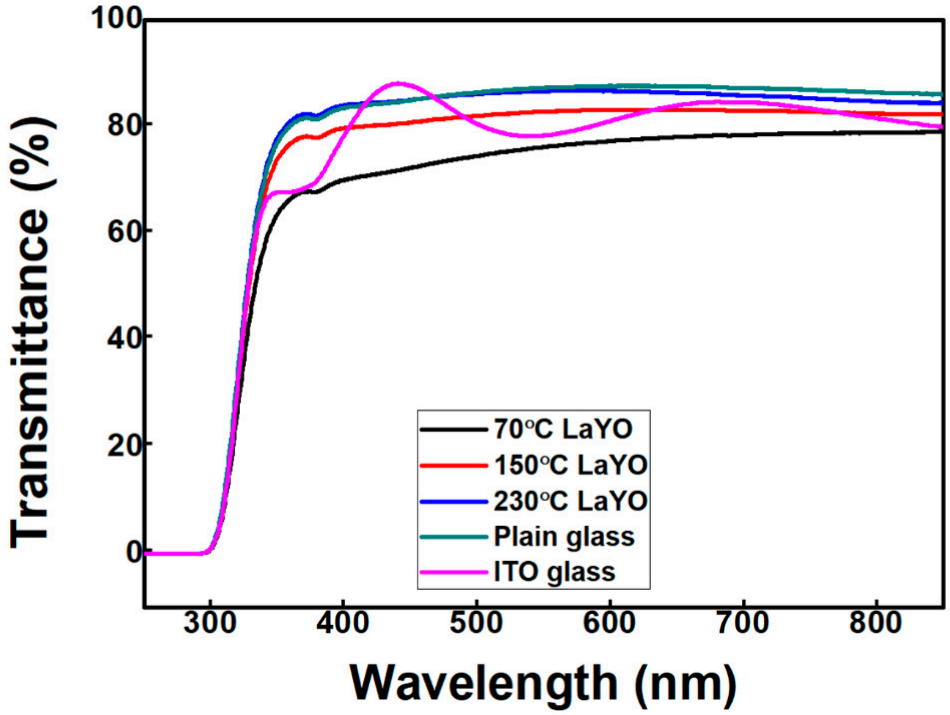

Figure 4. Optical transparency graphs acquired from the brush-coated nickel yttrium oxide films, plain glass, and indium-tin-oxide-coated glass.

The LC alignment state on the brush-coated NYO film was evaluated by POM measurements of AP LC cells assembled by the NYO films cured at 70, 150, and 230 °C. The corresponding POM results are represented in Figure 5a. The 70 and 150 °C cured sample-based LC cells revealed some defects and presented entirely yellowish images in POM when the polarizer and analyzer were vertically crossed. This signified instability of LC alignment and a light leakage effect of the LC cell, representing randomly distributed LCs on the NYO film. In contrast, the 230 °C cured sample-based LC cell exhibited a distinctly dark POM image without defects, indicating a uniform LC alignment state in the cell. The uniformly aligned LCs can guide the light unidirectionally, meaning that the polarized light from the polarizer could pass through the LC cell without any distortion. This light was blocked by the analyzer (placed after the LC cell), resulting in no light being observed in the POM measurement, as illustrated in Figure 5b.

The pre-tilt angle of LCs on the NYO alignment layer was investigated using the crystal rotation method via the oscillated transmittance curves of the LC cells, as depicted in Figure 6a [22,23]. The red line in the graph was obtained from the experimentally measured curve, whereas the blue line represented simulation data acquired from information on the LC cell gap and injected LCs in the cell. The 70 and 150 °C cured sample-based LC cells exhibited irregular experimental curves, which demonstrated a significant mismatch rate with the simulation data. This indicates an unstable LC distribution on the alignment layer; hence, the pre-tilt angle could not be obtained. In contrast, the 230 °C cured sample-based LC cell achieved a high match rate between the simulation and experimental data and the LC pre-tilt angle could be obtained (0.19°) with high reliability. This indicates a homogeneous LC alignment state on the NYO alignment layer. From the AFM, POM, and LC pre-tilt angle analysis, it was revealed that the directional anisotropic surface of the 230 °C cured NYO film could induce uniform and homogeneous LC alignment. With the nano/micro-grooved boundary of the surface, the LCs on the surface were constrained geometrically to the corresponding surface directionality, achieving uniform orientation [24–27]. The LCs have collective behavior characteristics and also fluidity, which are originated from the van der Waals forces between the LC molecules with accompanying elastic distortion. Hence, the surface LC molecules' orientation information is propagated to the LCs in the

cell, achieving uniform LC alignment in the cell. The LC alignment on the brush-coated NYO film is illustrated in Figure 6b.

The chemical affinity of the brush-coated NYO film surface was analyzed using contact angle measurements, as shown in Figure 7a. Here, deionized water and diiodomethane were used and their contact angles were reduced from 57.0° to 38.8° and from 55.3° to 44.3°, respectively, as the film curing temperature was increased from 70 to 230 °C. The surface energies of the samples were calculated using the Owen–Wendt method, as depicted in Table 1 [28]. The increase in surface energy indicated that the hydrophilicity of the NYO surface increased as the curing temperature increased. This can contribute to the homogeneous alignment of LC molecules on the surface, and corresponds to the LC pre-tilt angle analysis. The crystallinity of the 230 °C cured brush-coated NYO film was also analyzed using XRD, as shown in Figure 7b. In the range of 20–80 2-theta degrees, no distinct peak was observed, indicating that the NYO film has an amorphous structure. Although the solution-processed oxide film generally exhibited an amorphous structure below 500 °C curing [29], the 230 °C cured brush-coated NYO film achieved uniform LC alignment on the surface. Therefore, this demonstrated that the amorphous structure of the alignment layer did not affect the uniform alignment of the LC molecules.

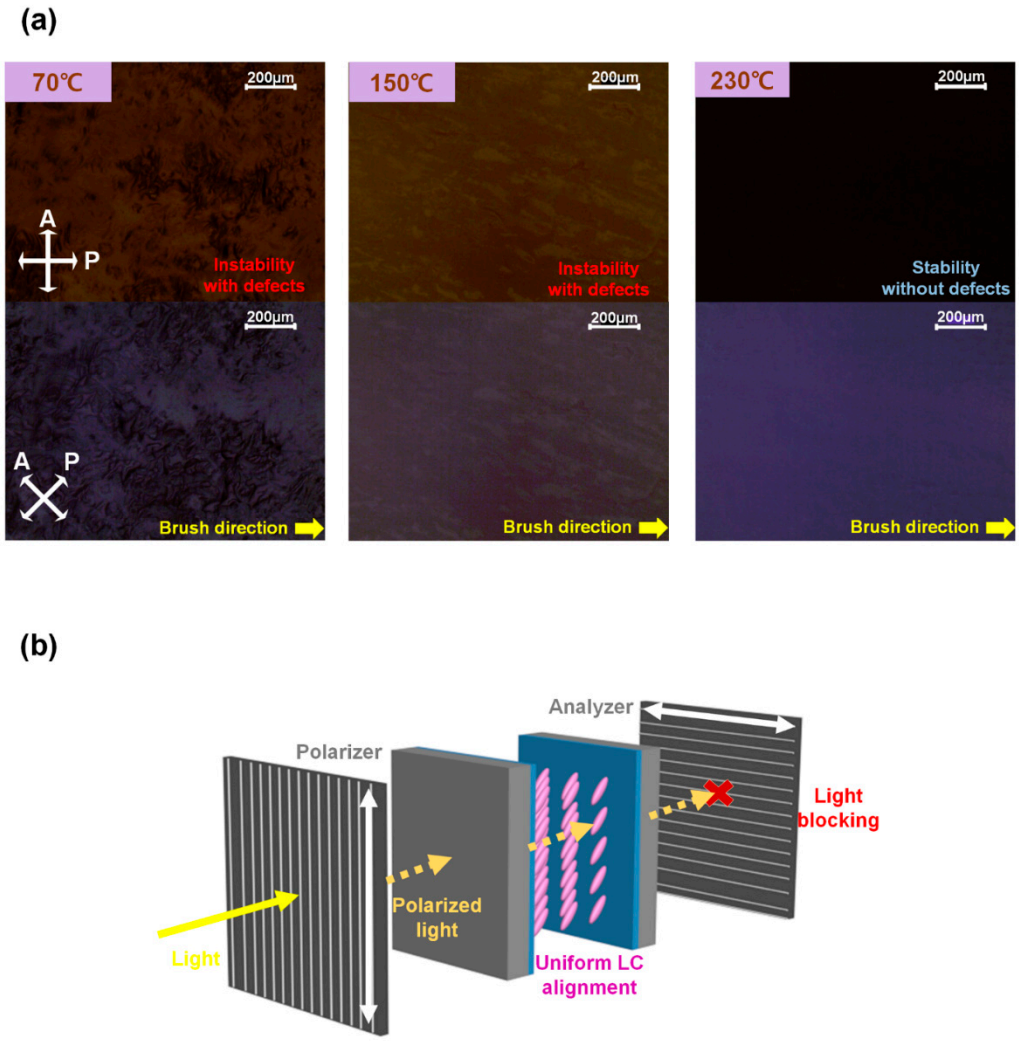

Figure 5. (**a**) Polarized optical microscopy results of anti-parallel liquid crystal (LC) cells made from brush-coated nickel yttrium oxide films cured at 70, 150, and 230 °C. The analyzer ("A") and polarizer ("P") directions are denoted by white arrows. (**b**) Schematic of light blocking process with uniformly aligned LCs in the cell.

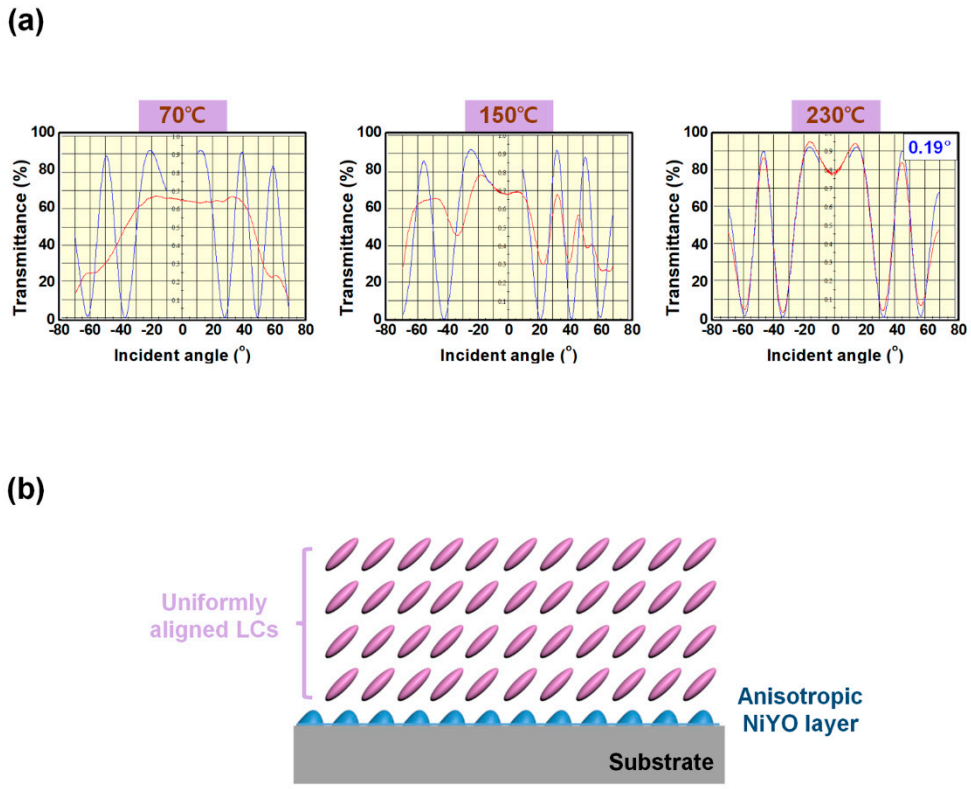

Figure 6. (**a**) Oscillated transmittance graphs measured from the anti-parallel LC cells based on the variously cured brush−coated nickel yttrium oxide films. The blue line denotes the simulation data, and the red line indicates the experimental data. (**b**) Schematic of the LC alignment on the anisotropic nickel yttrium oxide alignment layer.

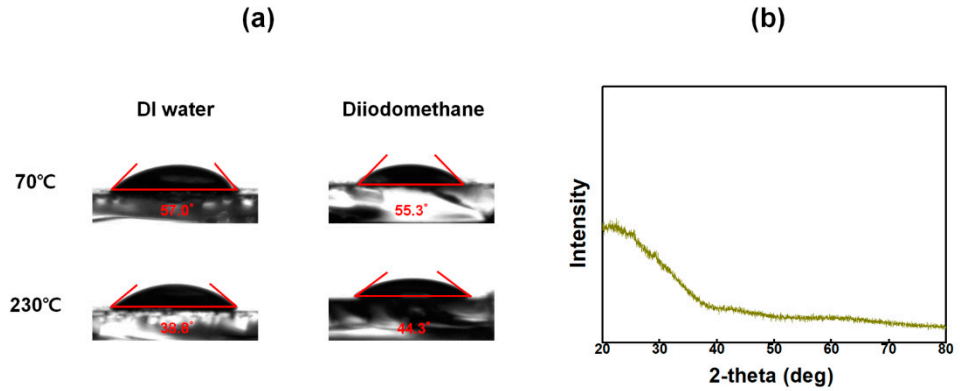

Figure 7. (**a**) Contact angle measurement results of the brush-coated nickel yttrium oxide films cured at 70 and 230 °C using deionized (DI) water and diiodomethane. (**b**) X-ray diffraction graph of the brush-coated nickel yttrium oxide film cured at 230 °C.

Table 1. Contact angles and surface energies of the brush-coated nickel yttrium oxide films cured at 70 and 230 °C.

Curing Temperature (°C)	Contact Angle (°)		Surface Energy (mJ/m^2)
	Deionized Water	Diiodomethane	
70	57.0	55.3	49.1
230	38.8	44.3	63.1

It is known that LC devices containing numerous switching components are subject to increasing temperature. Therefore, thermal stability of the alignment layer to uniform orientation of LCs is an significant factor in applications. Accordingly, the thermal endurance of the brush-coated NYO film to LC alignment was analyzed by the annealing process and POM measurements, as shown in Figure 8. Increasing temperature was applied from 90 to 180 °C at intervals of 30 °C. Uniform LC orientation state was verified by the POM results up to 150 °C. However, when the heat was increased to 180 °C, the POM result revealed defects, which indicated broken LC alignment. This result demonstrates the suitable thermal stability and potential of the NYO layer as an application to alignment layer of LCs compared to conventional PI layers [30].

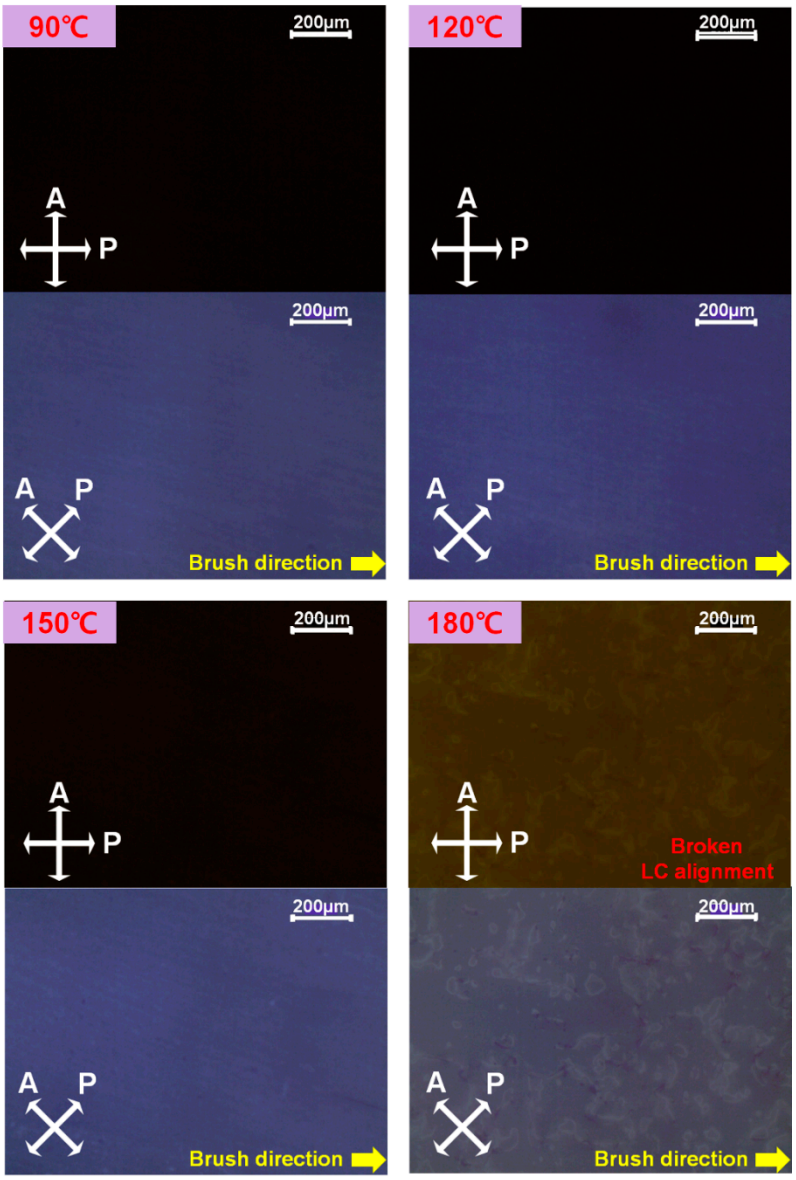

Figure 8. Thermal endurance of the brush-coated nickel yttrium oxide film to uniform LC alignment. Annealing was conducted from 90 to 180 °C at intervals of 30 °C for 10 min at each temperature.

The EO characteristics of the brush-coated NYO film were investigated using the R-T and V-T graphs, which were obtained from a TN-LC cell made from the NYO alignment layer. In the TN-LC system, the LCs in the cell converted their state between fall and rise depending on the applied external voltage. Moreover, the light transmittance could be controlled from this state transition. The R-T graph (Figure 9a) revealed the stable switching

performance of the NYO film-based TN-LC cell. The LC fall and rise state transition times were obtained to 13.7 and 3.6 ms in each, and the response time which obtained by the summation of rise and fall transition times was acquired as 17.3 ms. Moreover, the threshold voltage corresponding to 90% of optical transmittance was obtained as 0.9 V (Figure 9b). This value represents the enhanced voltage operating characteristic of the NYO film compared to that of conventional PI layers [31]. This also demonstrates the superior threshold voltage property compared to other recent studies of LC alignment layers [32,33]. Importantly, this low operating voltage results in low consumption of power. These results verified that the NYO film formed by brush-coating technique has a high potential for applications in TN-LC systems.

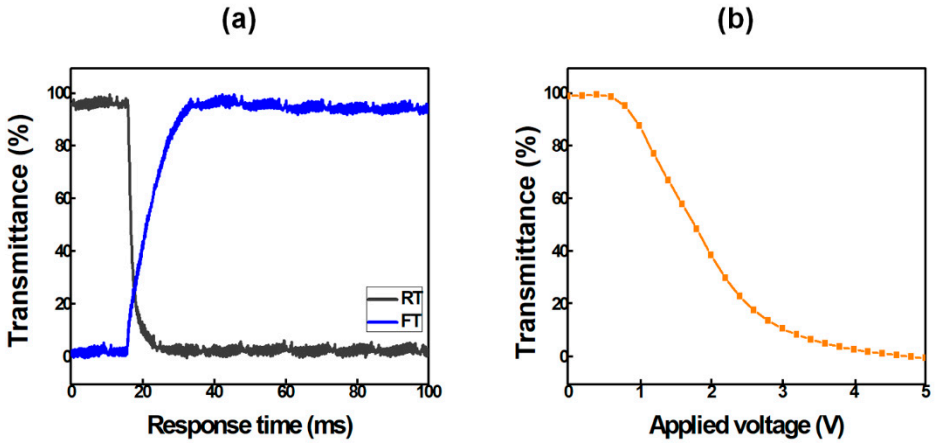

Figure 9. Investigation into electro-optical properties of twisted-nematic LC cell assembled from brush-coated nickel yttrium oxide films. (**a**) Response time and (**b**) threshold voltage.

4. Conclusions

An anisotropic NYO film surface was achieved using the brush coating method and was utilized as an LC alignment layer in this study. The NYO film was cured at 70, 150, and 230 °C after solution-processed brush coating, and the morphology of the formed films surface was investigated by AFM. The 230 °C cured film had a directional surface, and the XPS confirmed the well-formed NYO layer on the substrate. The directional surface was attributed to the shear stress, which was generated through the retracing force on the deposited solution. This nano/micro-grooved surface induced surface anisotropy, deriving uniform LC orientation on that. The homogeneous and uniform LC orientation state was demonstrated by POM and pre-tilt angle measurements. The NYO film achieved high optical transparency, and the contact angle analyses revealed an increase in hydrophilicity at higher curing temperatures. The LC cell fabricated by the NYO film exhibited suitable thermal endurance to LC alignment. Moreover, the NYO alignment layer also achieved good switching properties and enhanced operating voltage characteristics in a TN-LC system. Given these advantages, brush-coated NYO film has a high possibility for functional LC alignment layers.

Author Contributions: Conceptualization, D.-W.L.; methodology, D.-B.Y.; validation, D.-H.K.; formal analysis, D.-W.L.; investigation, J.-Y.O.; resources, D.-S.S.; writing—original draft preparation, D.-W.L.; visualization, J.-Y.O.; supervision, Y.L.; project administration, D.-S.S. All authors have read and agreed to the published version of the manuscript.

Funding: This research was supported by the National Research Foundation of Korea (NRF) grant funded by the Korea government (MSIT) (No. 2022R1F1A106419211).

Institutional Review Board Statement: Not applicable.

Informed Consent Statement: Not applicable.

Data Availability Statement: The data presented in this study are available upon request from the corresponding author.

Conflicts of Interest: The authors declare no conflict of interest.

References

1. Yan, X.; Mont, F.W.; Poxson, D.J.; Schubert, M.F.; Kim, J.K.; Cho, J.; Schubert, E.F. Refractive-index-matched indium-tin-oxide electrodes for liquid crystal displays. *Jpn. J. Appl. Phys.* **2009**, *48*, 120203. [CrossRef]
2. Li, J.; Wen, C.-H.; Gauza, S.; Lu, R.; Wu, S.-T. Refractive indices of liquid crystals for display applications. *J. Disp. Technol.* **2005**, *1*, 51. [CrossRef]
3. Lin, T.-H.; Jau, H.-C. Electrically controllable laser based on cholesteric liquid crystal with negative dielectric anisotropy. *Appl. Phys. Lett.* **2006**, *88*, 061122. [CrossRef]
4. Chen, Y.; Xu, D.; Wu, S.-T.; Yamamoto, S.; Haseba, Y.A. A low voltage and submillisecond-response polymer-stabilized blue phase liquid crystal. *Appl. Phys. Lett.* **2013**, *102*, 141116. [CrossRef]
5. Lee, J.J.; Park, H.G.; Han, J.J.; Kim, D.H.; Seo, D.-S. Surface reformation on solution-derived zinc oxide films for liquid crystal systems via ion-beam irradiation. *J. Mater. Chem. C* **2013**, *1*, 6824–6828. [CrossRef]
6. Garbovskiy, Y. Switching between purification and contamination regimes governed by the ionic purity of nanoparticles dispersed in liquid crystals. *Appl. Phys. Lett.* **2016**, *108*, 121104. [CrossRef]
7. Lee, W.-K.; Choi, Y.S.; Kang, Y.-G.; Sung, J.; Seo, D.-S.; Park, C. Super-fast switching of twisted nematic liquid crystals on 2D single wall carbon nanotube networks. *Adv. Funct. Mater.* **2011**, *21*, 3843–3850. [CrossRef]
8. Oh, S.-W.; Yoon, T.-H. Elimination of light leakage over the entire viewing cone in a homogeneously-aligned liquid crystal cell. *Opt. Express* **2014**, *22*, 5808. [CrossRef]
9. Outram, B.I.; Elston, S.J. Spontaneous and stable uniform lying helix liquid-crystal alignment. *J. Appl. Phys.* **2013**, *113*, 043103. [CrossRef]
10. Varghese, S.; Narayanankutty, S.; Bastiaansen, C.W.M.; Crawford, G.P.; Broer, D.J. Patterned Alignment of Liquid Crystals by μ-rubbing. *Adv. Mater.* **2004**, *16*, 1600. [CrossRef]
11. Kim, Y.J.; Zhuang, Z.; Patel, J.S. Effect of multidirection rubbing on the alignment of nematic liquid crystal. *Appl. Phys. Lett.* **2000**, *77*, 513. [CrossRef]
12. Ho, J.Y.L.; Chigrinov, V.G.; Kwok, H.S. Variable liquid crystal pretilt angles generated by photoalignment of a mixed polyimide alignment layer. *Appl. Phys. Lett.* **2007**, *90*, 243506. [CrossRef]
13. Ouchi, Y.; Lee, J.; Takezoe, H.; Fukuda, A.; Kondo, K.; Kitamura, T.; Mukoh, A. Smectic Layer Structure of Thin Ferroelectric Liquid Crystal Cells Aligned by SiO Oblique Evaporation Technique. *Jpn. J. Appl. Phys.* **1998**, *27*, L1993. [CrossRef]
14. Yaroshchuk, O.; Kravchuk, R.; Dobrovolskyy, A.; Qiu, L.; Lavrentovich, O.D. Planar and tilted uniform alignment of liquid crystals by plasma-treated substrates. *Liq. Cryst.* **2004**, *31*, 859. [CrossRef]
15. Haaren, J.V. Wiping out dirty displays. *Nature* **2001**, *411*, 29–30. [CrossRef] [PubMed]
16. Rao, K.V.; Smakula, A. Dielectric properties of cobalt oxide, nickel oxide, and their mixed crystals. *J. Appl. Phys.* **1965**, *36*, 2031. [CrossRef]
17. Tsutsumi, T. Dielectric properties of Y_2O_3 thin films prepared by vacuum evaporation. *Jpn. J. Appl. Phys.* **1970**, *9*, 735. [CrossRef]
18. Mell, C.C.; Finn, S.R. Forces exerted during the brushing of a paint. *Rheol. Acta* **1965**, *4*, 260. [CrossRef]
19. Kim, S.-S.; Na, S.-I.; Jo, J.; Tae, G.; Kim, D.-Y. Efficient polymer solar cells fabricated by simple brush painting. *Adv. Mater.* **2007**, *19*, 4410. [CrossRef]
20. Lee, D.W.; Kim, D.H.; Oh, J.Y.; Kim, D.-H.; Liu, Y.; Seo, D.-S. Tunable liquid crystal alignment and driving mode on lanthanum aluminum zirconium zinc-oxide thin film achieved by convenient brush-coating method. *ChemNanoMat* **2022**, *8*, e202200131.
21. Lee, D.W.; Kim, E.M.; Heo, G.S.; Kim, D.H.; Oh, J.Y.; Kim, D.-H.; Liu, Y.; Seo, D.-S. Oriented Yttrium Strontium Tin Oxide Micro/Nanostructures Induced by Brush-Coating for Low-Voltage Liquid Crystal Systems. *ACS Appl. Nano Mater.* **2022**, *5*, 6925. [CrossRef]
22. Han, K.Y.; Miyashita, T.; Uchida, T. Accurate measurement of the pretilt angle in a liquid crystal cell by an improved crystal rotation method. *Mol. Cryst. Liq. Cryst. Sci. Technol. Sect. A Mol. Cryst. Liq. Cryst.* **1994**, *241*, 147–157. [CrossRef]
23. Chen, K.-H.; Chang, W.-Y.; Chen, J.-H. Measurement of the pretilt angle and the cell gap of nematic liquid crystal cells by heterodyne interferometry. *Opt. Express* **2009**, *17*, 14143. [CrossRef] [PubMed]
24. Fukuda, J.-I.; Yoneya, M.; Yokoyama, H. Surface-Groove-Induced Azimuthal Anchoring of a Nematic Liquid Crystal: Berreman's Model Reexamined. *Phys. Rev. Lett.* **2007**, *98*, 187803. [CrossRef] [PubMed]
25. Kikuchi, H.; Logan, J.A.; Yoon, D.Y. Study of local stress, morphology, and liquid-crystal alignment on buffed polyimide surfaces. *J. Appl. Phys.* **1996**, *79*, 6811. [CrossRef]
26. Berreman, D.W. Solid Surface Shape and the Alignment of an Adjacent Nematic Liquid Crystal. *Phys. Rev. Lett.* **1972**, *28*, 1683. [CrossRef]
27. Chae, B.; Kim, S.B.; Lee, S.W.; Kim, S.I.; Choi, W.; Lee, B.; Ree, M.; Lee, K.H.; Jung, J.C. Surface morphology, molecular reorientation, and liquid crystal alignment properties of rubbed nanofilms of a well-defined brush polyimide with a fully rodlike backbone. *Macromolecules* **2002**, *35*, 10119. [CrossRef]

28. Adamson, A.W. *Physical Chemistry of Surfaces*, 5th ed.; Wiley-Interscience: Hoboken, NJ, USA, 1990.
29. Li, J.; Pan, Y.; Xiang, C.; Ge, Q.; Guo, J. Low temperature synthesis of ultrafine α-Al_2O_3 powder by a simple aqueous sol–gel process. *Ceram. Int.* **2006**, *32*, 587. [CrossRef]
30. Mun, H.-Y.; Jeong, H.-C.; Lee, J.H.; Won, J.-H.; Park, H.-G.; Oh, B.-Y.; Seo, D.-S. Poly(styrene–maleic anhydride) films as alignment layers for liquid crystal systems via ion-beam irradiation. *RSC Adv.* **2016**, *6*, 76743. [CrossRef]
31. Jeong, H.-C.; Lee, J.H.; Won, J.; Oh, B.Y.; Kim, D.H.; Lee, D.W.; Song, I.H.; Liu, Y.; Seo, D.-S. One-Dimensional Surface Wrinkling for Twisted Nematic Liquid Crystal Display Based on Ultraviolet Nanoimprint Lithography. *Opt. Express* **2019**, *27*, 18096. [CrossRef]
32. Wang, Y.-F.; Guo, Y.-Q.; Ren, Y.-X.; Fu, M.-Z.; Zhu, J.-L.; Sun, Y.-B. Study on polyvinylidene fluoride as alignment layer in twist-nematic liquid crystal display. *Liq. Cryst.* **2018**, *45*, 857. [CrossRef]
33. John V, N.; Rajeev, S.P.; Varghese, S. Ferroelectric polymer nanocomposite alignment layer in twisted nematic liquid crystal devices for reducing switching voltage. *Liq. Cryst.* **2019**, *46*, 736. [CrossRef]